Atmos. Chem. Phys. Discuss., 9, 17817–17849, 2009
www.atmos-chem-phys-discuss.net/9/17817/2009/

Atmospheric Chemistry and Physics Discussions

This discussion paper is/has been under review for the journal *Atmospheric Chemistry and Physics (ACP)*. Please refer to the corresponding final paper in *ACP* if available.

Transpacific pollution transport during INTEX-B: spring 2006 in context to previous years

G. G. Pfister[1], **L. K. Emmons**[1], **D. P. Edwards**[1], **A. Arellano**[1], **G. Sachse**[2], **and T. Campos**[1]

[1]National Center for Atmospheric Research, Boulder, CO, USA
[2]NASA Langley Research Center, Hampton, VA, USA

Received: 12 August 2009 – Accepted: 12 August 2009 – Published: 31 August 2009

Correspondence to: G. G. Pfister (pfister@ucar.edu)

Published by Copernicus Publications on behalf of the European Geosciences Union.

Abstract

We analyze the transport of pollution across the Pacific during the NASA INTEX-B (Intercontinental Chemical Transport Experiment Part B) campaign in spring 2006 and examine how this year compares to the time period for 2000 through 2006. In addition to aircraft measurements of carbon monoxide (CO) collected during INTEX-B, we include in this study multi-year satellite retrievals of CO from the Measurements of Pollution in the Troposphere (MOPITT) instrument and simulations from the chemistry transport model MOZART-4. Model tracers are used to examine the contributions of different source regions and source types to pollution levels over the Pacific. Additional modeling studies are performed to separate the impacts of inter-annual variability in meteorology and dynamics from changes in source strength.

Interannual variability in the tropospheric CO burden over the Pacific and the US as estimated from the MOPITT data range up to 7% and a somewhat smaller estimate (5%) is derived from the model. When keeping the emissions in the model constant between years, the year-to-year changes are reduced to (2%), but show that in addition to changes in emissions, variable meteorological conditions also impact transpacific pollution transport. We estimate that about 1/3 of the variability in the tropospheric CO loading over the contiguous US is explained by changes in emissions and about 2/3 by changes in meteorology and transport. Biomass burning sources are found to be a larger driver for inter-annual variability in the CO loading compared to fossil and biofuel sources or photochemical CO production even though their absolute contributions are smaller. Source contribution analysis shows that the aircraft sampling during INTEX-B was fairly representative of the larger scale region, but with a slight bias towards higher influence from Asian contributions.

ACPD

9, 17817–17849, 2009

1 Introduction

Over the past decade, the pollution transport between continents has received increased attention due to the potential impact on the air quality of continents downwind. Special attention has been given to the transport of pollutants between Asia and North America because of the rapid development of countries in Asia and the potential offset of increasing Asian emissions on emission controls within the US (Park et al., 2005). Transport of pollution across the Pacific is well documented in the literature (e.g. Jaffe et al., 2004; Goldstein et al., 2004; Parrish et al., 2004) and has been the objective of various field campaigns. Bey et al. (2001) examined aircraft data from the NASA Pacific Explatoratory Mission (PEM)-West B mission in February–March 1994 and found that frontal lifting of pollution over central and eastern China ahead of eastward moving cold fronts, followed by westerly transport in the lower free troposphere was the principal process for export of anthropogenic and biomass burning pollution from Asia. Similar findings were made by Liu et al. (2003) who focused their analysis on the Transport and Chemical evolution over the Pacific (TRACE-P) aircraft campaign (February–April 2001). Wang et al. (2006) found that meteorology is most conducive to transpacific transport in the lower troposphere during early spring (March–April) and in the mid-to upper troposphere in May. Other studies showed that Asian outflow might also be mixed with contributions from intercontinental transport with European and North-African sources making a major contribution (Newell and Evans, 2000; Bey et al., 2001).

Even though the pollution transport across the Pacific has been the focus of various studies, uncertainties remain such as in understanding to what degree the interannual variability is impacted by different drivers, including changes in emissions, transport pathways and the oxidizing capacity of the atmosphere. Szopa et al. (2007) analyzed surface measurements of CO for 1997–2001 together with modeling tools and found that for latitudes above ~60° N the CO inter-annual variability is controlled almost equally by variations in biomass burning emissions and meteorology, while they

ACPD
9, 17817–17849, 2009

found meteorology to be the driving factor in the tropics.

In this paper we combine aircraft measurements of carbon monoxide (CO) collected over the Pacific and the US West Coast during the NASA Intercontinental Chemical Transport Experiment Part B (INTEX-B) in spring 2006 with the multi-year data series of MOPITT CO and accompanying model simulations from a global chemistry transport model to analyze the inter-annual variability in pollution transport across the Pacific. CO has a lifetime of the order of weeks, which makes it a well-suited tracer for pollution transport. It is produced by incomplete combustion of fossil fuels and biomass, and by oxidation of methane and other hydrocarbons and is destroyed by oxidation of OH.

We use observed and modeled tropospheric CO loadings to examine how representative pollution transport during INTEX-B was in the context of previous years, and we use model CO tracers for specific source types and source regions to relate the airmass origins of the aircraft measurements to the larger scale picture. Model experiments are further used to estimate the relative roles of changes in emissions versus changes in meteorology and dynamics on interannual changes in pollutant transport. Knowledge about the relative importance of the "natural" variability in the CO burden is essential for regulatory purposes such as testing emission control strategies or for trend analysis.

2 Observations and modeling

2.1 In-situ and satellite observations

The second part of the NASA INTEX-B aircraft campaign took place during 15 April–15 May 2006 with the objective of characterizing the transpacific transport and evolution of Asian pollution on its way to North America (Singh et al., 2009). We make use of 1 min averaged CO data sampled on board the NASA DC8 and the NCAR/NSF C-130 aircrafts. CO measurements on the DC-8 were made by a fast response tunable diode laser (TDL) instrument (Sachse et al., 1987). The measurement precision is given as

ACPD
9, 17817–17849, 2009

1% or 1 ppb whichever is greater. A vacuum UV resonance fluorescence instrument similar to that of Gerbig et al. (1999) is used to measure CO on the C-130. Data have 3 ppb precision and accuracy is better than 10% for a 100 ppb ambient CO mixing ratio. During April, the DC-8 aircraft was operated out of Hawaii with 3 local science flights, and during May out of Anchorage, AK with 4 local science flights. The C-130 was operated out of Seattle, WA during this time period, conducting 10 local science flights.

Retrievals of CO from the Measurements of Pollution in the Troposphere (MOPITT) instrument (Drummond et al., 1996; Deeter et al., 2004) have been available since March 2000. Due to a cooler failure, no retrievals are avalaible for May to August 2001. For the analysis presented here we use the monthly gridded Level 3 product for the recently released Retrieval Version 4 (V4). Validation of V3 retrievals has been performed on a regular basis since the start of the mission (Emmons et al., 2004, 2007, 2009a) and first validation results for the V4 product are presented on the MOPITT Homepage (http://www.acd.ucar.edu/mopitt/). In our analysis we limit the MOPITT data to daytime retrievals since retrieval sensitivity is generally greater for daytime compared to nighttime overpasses.

2.2 Model simulations

We use version 4 of the MOZART chemistry transport model, which is described and evaluated in greater detail in Emmons et al. (2009b). Modifications from Version 2 published in Horowitz et al. (2003) include, amongst others, a more complete description of anthropogenic hydrocarbon chemistry, the inclusion of tropospheric aerosols (extended from the work of Tie et al., 2001, 2005), and on-line calculations of photolysis rates, dry deposition, H_2O, and biogenic emissions (Pfister et al., 2008).

The model was run at a horizontal resolution of ~2.8° by 2.8° (T42). The meteorological fields for 2004 for driving MOZART were taken from NCEP (National Centers for Environmental Prediction)-NCAR-Renalysis and were regridded to the model resolution and interpolated from a 6-h time structure to the 20 min time steps of the simulations. The vertical resolution of the model consists of 28 hybrid levels between the

ACPD
9, 17817–17849, 2009

surface and 2 hPa (~45 km).

The multi-year model simulations cover the years 2000 through 2006 with monthly average output and the INTEX-B specific time period (March through May 2006) with output of 3-h average concentration fields. We included a tagging scheme in the model, which allows estimating the contributions of various source terms to atmospheric CO concentrations. We keep track of a total of 18 CO tracers including CO from biomass burning sources (BB), anthropogenic (fossil fuel and biofuel use; FF) and direct biogenic sources from soil, vegetation and ocean (BIO) for each of six regions in the Northern Hemisphere: Europe and North Africa (EuAf) [0–75° N, 20° W–60° E], SW Asia (SWAs) [0–45° N, 60–100° E], SE Asia (SEAs) [0–45° N, 100–180° E], North Asia (NAs) [45–75° N, 60–180° E], North America (NAm) [30–75° N, 180° W–20° W], Mexico and Central America (CAm) [0–30° N, 180° W–20° W]. The three Asian regions combined are referred to as ASIA. Regional CO tracers are defined as CO^{EuAf}, CO^{SWAs}, etc., and if tracers are also separated by source type, then the CO label is exchanged by the corresponding sources type acronyms, e.g. FF^{EuAf}, BB^{ASIA}, etc. Where FF and BB sources are combined for a region, the corresponding acronym is FFBB. CO from photochemical production (CO^{CHEM}), which is not tagged separately in the simulations, is estimated from the difference between total CO and the sum over all tracers. This estimate is impacted by contributions from non-tagged sources including oceanic emissions and sources in the Southern Hemisphere but their contributions are expected to be small for the regions where we focus our analysis.

In addition to the standard simulation with inter-annual varying emission strength ("MozVar"), we performed a simulation in which we kept emission levels for all years constant at the 2006 levels ("MozConst"). The combined analysis of these two simulations allows estimating the impacts of meteorology versus emissions on the inter-annual variability in the tropospheric CO loading.

ACPD
9, 17817–17849, 2009

2.3 Multi-year emissions

Biofuel and fossil fuel emissions for the globe were taken from the European Union project POET (Precursors of Ozone and their Effects in the Troposphere) (Olivier et al., 2004) and for Asia from Ohara et al. (2007). Biomass burning emissions for 2000-2006 are from the Global Fire Emission Data Base Version 2 (GFED-v2) (van der Werf, 2006).

Table 1 lists emission totals for CO for March through May of the individual years. The Asian anthropogenic inventory includes year-to-year changes and reflects the strong increase in industrialization in this part of the globe (Ohara et al., 2007) with a 13% increase in CO emissions over 2000–2006. These emissions are within the range of other inventory such as the study by Zhang et al. (2009) who estimate Asian emissions for the entire year 2006 as 298.2 Tg CO with an 18% increase from 2000 to 2006. The anthropogenic emissions used for the remainder of the globe as well as the biogenic direct CO emissions refer to a single year (2000) only, and as a result, the simulations might underestimate the corresponding year-to-year variations.

BB sources are generally smaller in magnitude compared to FF, but show the largest year-to-year variability with emissions changing by up to a factor of 2–3 between years. Most biomass burning emissions during springtime originate from the mid and low latitudes and fire activity in the boreal zones is generally low. However, 2003 was an exceptional year when fires in Siberia started unusually early in the season and with very high intensity increasing biomass burning emissions for the entire Asia region to nearly 50% above average (Edwards et al., 2004). March through May total BB emissions for N-Asia (>45° N) are in the order of 6–12 Tg CO, except for 2003 when they reach an estimated 39 Tg CO. For comparison, BB sources in S-Asia (<45° N) are in the range 14–34 Tg CO.

Most biomass burning emissions for the N-American region during spring originate from the lowermost latitudes (CAm region), and strongest fire activity is seen for the years 2000 and 2003 with emissions up to twice above normal. BB emissions for the

ACPD
9, 17817–17849, 2009

continental US and Canada account for only a small part of these totals (of the order of about 1 Tg CO for latitudes >30° N compared to 4–28 Tg for latitudes <30° N).

CO loadings during springtime are a result of recent emissions, but also result from CO accumulating during wintertime when CO lifetime is of the order of a few months. The modeled variability in FF emissions for wintertime months is comparable to springtime. Asian and North American BB emissions for wintertime are generally less compared to springtime and will contribute less to springtime variability. E.g. Asian BB emissions for December–February are in the range 3–17 Tg compared to 29–53 Tg for March–May. From these results we conclude that the emission estimates for spring 2006 are in the average range of estimates over the 2000–2006 time frame.

2.4 Model evaluation

We evaluate the performance of the modeled CO fields during the INTEX-B time period by comparison to aircraft data. For the multi-year period we evaluate the model results by comparison to MOPITT CO retrievals.

For comparison to INTEX-B aircraft data, we interpolated the 3 h model field to the time, location and altitude of the aircraft. Average vertical observed and modeled CO profiles and their absolute difference for April and May flights for the DC-8 and C-130 aircraft are illustrated in Fig. 1. The model, in all cases, gives a good representation of the magnitudes and vertical shape. Absolute differences are generally within 10 ppb. The largest difference is seen for the lowest altitude bin for the C-130 flights in May when the model is higher by ~30 ppb. However, in this case we also find the highest variability in observed and modeled CO values. During the May phase of the campaign, the C-130 performed six science flights with a high number of low altitude legs over land. Thus, observations were more impacted by local emissions and processes, which are less well represented in the global model. In comparison, four science flights were performed during the April phase with three of them mostly out over the ocean.

Figure 2 shows springtime CO total columns from MOPITT and corresponding MOZART simulations over the Northern Hemisphere averaged over the years 2000–

ACPD
9, 17817–17849, 2009

2006. The monthly mean MOPITT averaging kernels and a priori information have been applied to the model concentrations fields. The two boxes in this Figure denote the regions on which we focus in the following analysis. The one region over the Pacific Ocean ("PAC") is chosen as being overall representative of the transport of pollution from Asia to North America, the other ("US") is chosen as being representative of the impact of transpacific pollution transport on the contiguous US.

Compared to MOPITT, MOZART gives a good representation of the spatial characteristics with a correlation coefficient (r^2) of 0.89 for the entire Northern Hemisphere, 0.97 over PAC, and 0.92 over US. The model overall matches springtime MOPITT CO fairly well with mean biases over the different regions of 2±7%, −1±2%, and −0.5±3%, respectively.

While some of the disagreement is due to uncertainties in the emission estimates, especially close to source regions, and the modeled transport and chemistry, some part can also be explained by different temporal sampling between MOPITT and the model in forming monthly means. While we do output a true monthly mean from the model, the MOPITT monthly mean calculation is impacted by gaps in the coverage and by missing data.

Uncertainties in the retrieval should also be considered in the disagreements. Emmons et al. (2009a) find a 19% positive bias for V3 column retrievals determined by validation with in-situ measurements from aircraft during INTEX-B. From comparisons to long-term records of CO measurements they state that the bias may have been increasing over time. The newly released MOPITT retrieval version (V4) (Deeter et al., 2007; Emmons et al., 2009a), however, shows a significantly smaller bias bias (<1% for retrievals at 700 hPa) and less drift (~1 ppb/yr at 700 hPa) (Merritt et al., 2009).

3 Discussion

We use the aircraft and MOPITT data together with model simulations to analyze the source contributions and the inter-annual variability in the tropospheric CO burden over

the Pacific and North-America. The goal of this analysis is to place the CO budget for spring 2006 into the context with previous years.

3.1 Inter-Annual variability in total CO and tracers

In Fig. 3 we compare the inter-annual variability in the CO burden as derived from MOPITT and corresponding results from the two model simulations MozVar and MozConst. In support of the analysis, Table 2 lists the modeled source contributions for the springtime CO burden over the PAC and US regions from the MozVar simulation. The CO burdens were integrated over the altitude range 800–300 mbar to be most representative of the typical MOPITT vertical sensitivity. To show the effects of applying the MOPITT averaging kernels, Fig. 3 gives results for MozVar when the burden is calculated without consideration of the MOPITT averaging kernels and data coverage (labeled as MozVar_noAK). These are very similar to results when the satellite retrieval characteristics are considered, and confirm the validity of using a simple altitude integration for the tagged sources.

From Table 2 we estimate the average source contributions to the CO burden for the regions of interest. Over PAC, BB sources account on average for 12% (3.8 Tg) versus 42% (12.8 Tg) for FF, and 4% (1.2 Tg) for biogenic CO. ASIA is the source region contributing the most (34% or 10.4 Tg), followed by EuAf (14% or 4.2 Tg) and Nam (8% or 2.6 Tg). Non-tagged sources, which are mostly composed of CO produced photochemically and minor contributions from untagged direct emissions such as the Southern Hemisphere or aircraft emissions, explain 42% (12.9 Tg). Similar relative source type contributions are found for the US: 11% (2.1 Tg) from BB, 45% (8.5 Tg) from FF, and 5% (0.9 Tg) from BIO. The role of NAm sources for the US increases to 16% (3.0 Tg), but ASIA still shows the largest contribution (28% or 5.3 Tg). Similar relative source contributions are calculated when the budget is extended to the entire tropospheric range (surface to 100 mbar).

The year-to-year changes in the MOPITT data (Fig. 3) are in the range of −7% to +4% over PAC and −5% to +4% over US. MozVar picks up the overall features in the

ACPD
9, 17817–17849, 2009

year-to-year variability fairly well, but gives a slightly smaller range (−5% to +4% and −3% to +5%, respectively). Inter-annual variations in MozConst range from about −2% to +2% for both regions. Even though this is less than the range found from MozVar, it demonstrates that in addition to the variability in direct emissions, changes in the meteorology also can impact the tropospheric CO loading noticeably.

From the source type analysis in Table 2 we find that a large part of the inter-annual variability is driven by changes in the BB source, even though it contributes less to the total CO burden than FF. The FF tracer burden shows an overall increase over time, which is driven by the increase in Asian sources. The smaller year-to-year variability superimposed on this increase reflects the impact of changes in dynamics and meteorology, discussed in the following section.

PAC and US show similar patterns in inter-annual variability as influenced by the weeks-long lifetime of CO and its widespread transport. The first two years of the time period, 2000 and 2002, are below average, and later years generally above the 2000–2006 average. 2002 shows the largest negative deviation from the 6 yr mean of −7% in the MOPITT data over PAC. MozVar also estimates below average values, but gives similar deviations for 2000 and 2002 (∼−4%). These years are also below average for the US. The low CO loadings are related to a rather low biomass burning activity in Asia and some of the lowest Asian anthropogenic emissions for the time period considered (Tables 1 and 2). Results from the MozConst simulation indicate, that variations in the meteorology and transport have contributed to below average values for the selected regions as well.

Spring 2003 is strongly impacted by biomass burning in Northern Asia (Tables 1 and 2) and shows a strong positive deviation in both MOPITT and model (+4%). These fires not only impacted PAC, but also contributed to a positive deviation over the US region. The major part of the enhancement in total CO for this year over PAC (and to a large part US as well) is explained by the large North Asian fire tracer contribution.

For the latter part of the time period considered (2004–2006), the MOPITT analysis gives mostly positive deviations on the order of 1–4% over PAC and 1–3% over US

ACPD
9, 17817–17849, 2009

with largest loadings for 2005. The modeled variability does not follow the observed patterns in every case. The model identifies the largest positive deviation also for 2005 over the US (+2%), but simulates the largest positive deviation over PAC in 2004 (3% in 2004 versus 1% for 2005). However, the model captures the overall features and variability seen in the MOPITT data and represents the major events. Model simulations and MOPITT data support the conclusions drawn from the analysis of the emission inventories and indicate that in relation to the previous six years, spring 2006 is reasonably representative of a "typical" springtime CO loading over the Pacific or North America.

3.2 Variability in the CO burden in relation to changes in meteorology and emissions

We apply a combined analysis of concentration fields from MozVar and MozConst to estimate the relative importance of changes in emissions versus changes in meteorology on the interannual variability in the tropospheric CO burden. For this purpose we contrast for each grid cell over the area of interest the absolute deviation from the mean value in the total and tagged CO burden (surface-100 mbar) between the two model simulations MozVar and MozConst (Fig. 4). For this portion of the analysis we average the burden over April–May for each of the seven years for each model grid cell within either PAC or US.

The variability in the total CO loading is on the order of 2 Gg CO (2%) in MozConst, which is about half of that found from Mozvar for PAC (~4 Gg or 5%), and about 1/3 of that found for US (3 Gg or 3%). From this we estimate that roughly 1/3 of the variability over US might be explained by changes in emissions and about 2/3 by variable meteorology. Over PAC changes in emissions and changes in meteorology contribute with roughly equal parts. These relations are comparable to the findings from Fig. 3 and similar sensitivities were found by Szopa et al. (2007). Since FF sources others than for Asia are kept constant in the model, we expect that our estimates slightly underestimate the impact of changing emissions.

ACPD
9, 17817–17849, 2009

CO^{CHEM}, which explains about half of the CO load, has a variability of ~0.5 Tg (1–2%) and does not change significantly whether emissions are held constant or vary from year-to-year. For CO from direct tagged emissions, which make up for roughly the other half, we find a clear increase in the variability when year-to-year changes in the source strength are considered. Summing up all model tracers we find the variability increasing from 1.5 Tg (3%) to 3 Tg (7%) over PAC and 1.8 Tg (4%) to 2.6 Tg (5%) over US, respectively.

The BB tracer, which contributes to the CO budget with roughly 10%, shows the largest change between MozConst and MozVar: 2.4 Tg (25%) over PAC and 1.3 Tg (15%) over US for MozVar compared to less than 0.5 Tg (3–5%) for MozConst. FF tracers with contributions about four times as large as those for BB, give a standard deviation of close to 2 Tg (5%) in MozVar, which is only slightly larger than the variability in MozConst. The biogenic tracer changes only slightly between MozVar and MozConst as expected since in the model the source strength is held constant from year to year. In regard to regional tracers, we find the largest variability increase for Asian FFBB sources. For this tracer, inter-annually varying emissions increase the variability by about a factor of 3. Less impact is seen for $FFBB^{NAm}$ and $FFBB^{CAm}$ (factor 2 or less increase) and only minor changes for the European and African tracers over the regions of interest.

In Fig. 5 we analyze the degree to which individual tracers contribute to the variability in the total CO burden. For this purpose we calculate the correlation between the absolute variability in individual tracers and the total CO burden. Over PAC we find that with constant emissions the FF source (mostly from Asian source regions) can explain the major part of the variability, while with inter-annually varying emissions the BB source (again mostly from Asian source regions) plays the major role. For US, even though the BB source (again mostly from Asian sources) gains in importance relative to the FF source (in this case from NAm sources), the latter still remains the main contributor. Similar to FF, the BIO tracer shows a higher correlation for MozConst compared to MozVar. It is also interesting to note that for both PAC and US biomass

ACPD
9, 17817–17849, 2009

burning from Northern Africa, which makes for the major part of the BB^{EuAF} tracer burden, has a rather high correlation in MozVar. Thus, even though BB sources in general contribute less to the atmospheric CO loading, they dominate year-to-year changes in CO.

The connections to the emissions themselves is shown in Fig. 6, where information about the variability in CO tracer burden contributions is combined with information about the variability in the respective source strength of the CO tracers. Over PAC, the largest tracer contributions are from FF^{ASIA}, FF^{EuAf} and BB^{ASIA}, with the two Asian tracers amongst the sources that have the largest year-to-year variability. For US, also FF^{ASIA} is the major contributor, but it is only slightly more important than the FF^{NAm} tracer, for which the emission estimates do not change between years. Hence, the main contributing sources to the CO load over US exhibit a smaller year-to-year variability and the relative importance of changes in emissions versus changes in meteorology on the tropospheric CO loading is for this reason less pronounced compared to PAC (Fig. 4).

3.3 Variability and its effect on detecting trends

We use the information about the inter-annual variability from the MozConst simulation to estimate how such a "natural" variability would impact the detection of a possible trend in emissions. For a simple theoretical estimation based on values for PAC we assume that the burden at the beginning of a 7 yr long time period is 50 Tg (CO burden integrated from the surface to 100 mbar) and that a source change introduces a 0.5 Tg increase per year in the total burden. Without considering additional triggers of variability, a linear fit to this timeseries results in a slope of 0.5 Tg yr^{-1} (0.98% yr^{-1}).

In order to consider the "natural variability" we superimpose the variability derived from MozConst (compare to values shown in Fig. 3). In this case a linear trend calculation gives a slope of 0.81±0.1 Tg yr^{-1} (1.6±0.2% yr^{-1}), which overestimates the actual trend by ~50%. From Fig. 3 we see that the time series of the variability ac-

ACPD
9, 17817–17849, 2009

tually supports an increasing trend and such a feature could cause a serious issue in trend studies, where variability is expected to be random. This is especially true if only a rather short time period is availale for analysis. If, e.g., we reverse the temporal order of the superimposed trend, then the estimated slope results in an underestimate of the actual trend: $0.19\pm0.1\,\mathrm{Tg\,yr^{-1}}$ ($0.4\pm0.2\%\,\mathrm{yr^{-1}}$). It would require a time series over three times this time period (~21 yr) for the "natural variability" to become sufficiently random and to derive trends close to the exact value: $0.54\pm0.03\,\mathrm{Tg\,yr^{-1}}$, and $0.46\pm0.03\,\mathrm{Tg\,yr^{-1}}$, respectively. These results demonstrate the importance of considering sufficiently long data series for trend analysis and raise the issue that "natural" variability might not necessarily be considered random.

3.4 Representativeness and budget analysis for INTEX-B campaign data

We compare the source contributions for the DC-8 and C-130 science flights to source contributions for suitable larger regions and monthly averages to examine how representative the selected flight patterns and times are in a larger picture. Source contributions for the flight tracks are estimated by mapping modeled concentrations to the time and location of the aircraft. Transit flights have been excluded from this analysis.

In Fig. 7 we show the source contributions for vertical average CO profiles. Because of the different focus regions of the DC-8 in April and May, we treat the two months individually. The average contributions for the DC-8 flight tracks in April are compared to a flight representativeness region ("HAwaii"), which is defined by an area covering all the flight tracks (175–155° W, 20–45° N). For May, when the DC-8 was operating out of Anchorage, the representativeness region is defined as 175° E–135° W and 40–65° N ("AK"). The C-130 operated out of Seattle during both months and the representativeness region is defined from 135–115° W and 35–55° N ("SEattle"). In addition, comparisons to the larger PAC and US regions defined earlier are included as well. In support of the analysis we show in Fig. 8 maps of the average springtime tropospheric CO loading and various tracer contributions.

Average total CO concentrations for DC-8 in April out of Hawaii range from 135–

145 ppb peaking at ~7 km (Fig. 7). The largest contributors are CO^{CHEM} and FF^{ASIA}. CO^{CHEM} ranges from 51 ppb (~38% of total CO) to a maximum of 57 ppb at 7 km (or 42% at 9 km). FF^{ASIA} values range from 34–45 ppb (~25–31%) and BB^{ASIA} from 6–13 ppb (4–9%). The Asian tracers show the maximum concentrations around 5–7 km. In contrast, the N-American tracer shows the strongest signals at low altitude (14 ppb or 11%), and values are decreasing to 7–8 ppb or 5–6% at the higher altitudes. CO from EuAf sources is highest at the low altitude bin, concentrations range from 23 ppb (17%) to 12 ppb (9%). CAm sources contribute with about 2 ppb (1–2%), and the biogenic tracers with 5–6 ppb (4%).

Comparison with HA shows that the DC-8 flights fairly well represent the larger region and monthly mean. The different tracers show similar vertical structure, absolute values for the DC-8 are somewhat higher, mostly due to higher contributions from Asian sources. The main difference is at about 7 km with total CO higher by 16 ppb. This is mostly due to higher FF^{ASIA} (9 ppb) and BB^{ASIA} (3 ppb) and can be related to the target of the campaign being set on sampling Asian outflow and actively seeking out pollution plumes. CO^{CHEM} at higher altitudes is larger by 3–4 ppb for DC-8 compared to HA. The relative tracer contributions agree to within 3% between the DC-8 and HA. HA relative budgets agree with the larger PAC region to within 1–2% with somewhat smaller contributions from Asian sources and somewhat higher contributions from NAm and CAm sources.

For the DC-8 flights in May out of Anchorage, total CO ranges from 150–110 ppb with values decreasing with altitude. Again the largest contributors are CO^{CHEM} (43–53 ppb) and FF^{ASIA}. Maximum values for FF^{ASIA} are now found at lower altitudes (37 ppb or ~26% at 3–5 km). $FFBB^{NAm}$ and $FFBB^{EuAf}$ range from 17–11 ppb and 27–15 ppb and, as before, show largest values at low altitudes. When compared to the larger AK region, both budgets show similar vertical structure in total CO, but DC-8 features higher values by about 1 ppb at the lowest altitude and up to 11 ppb for 3–5 km. We find higher tracer values for FF^{ASIA} (up to 6 ppb at 5 km), CO^{CHEM} (up to 5 ppb at 9 km),

ACPD
9, 17817–17849, 2009

and $FFBB^{NAm}$ and $FFBB^{EuAf}$ (1–2 ppb). BB^{ASIA} in DC-8 is comparable between the two budgets except for the lowest altitude where it is 5 ppb lower in DC-8. Individual relative contributions are within ~3%.

AK and PAC relative contributions differ more than the relative contributions between HA and PAC. AK shows generally a higher CO loading and largest differences in the relative terms are seen for CO^{CHEM} which contribution, due to the high latitude, is up to 6% smaller in AK compared to PAC. Other tracer contributions agree to within 3%, with 2–3% smaller contributions for NAm and EuAf.

The comparison for C-130 flight tracks with the larger SE region is shown in Fig. 7 for April and May separately, and in Table 3 for an average over both months. In April, the largest contributors to the C-130 values are CO^{CHEM} (54–47 ppb or 34–38%), FF^{ASIA} (31–45 ppb or 21–32%), $FFBB^{NAm}$ (13–26 ppb or 10–17%), and $FFBB^{EuAf}$ (19–25 ppb or 14–16%). Similar to the DC-8 flights, FFBB tracers for NAm and EuAf have largest values for the low altitude bins, while the Asian tracers are largest at high altitudes.

Regionally averaged absolute CO concentrations are generally lower in May, partly due to increased photochemical loss of CO. At the lowest altitude the total average CO for C-130 flight tracks, however, is highest in May. This is explained by the more frequent sampling of air masses over the continent near emission sources for May flights compared to April flights (Sect. 2.4). $FFBB^{NAm}$ explains 13 ppb of the difference, and there is also a slightly higher influence of Asian plumes (FF^{ASIA} and BB^{ASIA} are larger by 2 and 3 ppb, respectively).

Total CO for the C-130 flight tracks in April agrees to within 5 ppb with SE, except for the 7 km bin where C-130 is higher by 11 ppb, which is mostly due to higher FF^{ASIA} values. C-130 averages for total CO for May flights are larger than SE at all altitudes. A bias of 27 ppb bias at the lowest altitudes is mostly explained by higher values of $FFBB^{NAm}$ (17 ppb), i.e. again a reflection of the large number of flight tracks over the continent, $FFBB^{EuAf}$ (4 ppb) and FF^{ASIA} (5 ppb), the latter an indication of targeting Asian outflow. At the higher altitudes it is the FF^{ASIA} tracer explaining the major part of

ACPD
9, 17817–17849, 2009

differences (9 ppb at 7 km) followed by $FFBB^{EuAf}$ (4 ppb).

When flights are averaged over April and May (Table 3), the total CO for C-130 is larger compared to SE at all altitudes. The largest differences are at the highest altitude bin (14 ppb), where FF^{ASIA} explains the major part (9 ppb), and at the lowest altitude (12 ppb), in which case $FFBB^{NAm}$ is the major factor (8 ppb). Comparing SE to the larger US regions we find clearly larger CO loadings at the lowermost altitudes mostly due to higher contributions from NAm. Relative NAm contributions over SE range from 17% at the lowest altitude bin to 9% at the highest altitude bin. Over US the range is from 31% to 11%, respectively. Asian contributions range from 26–33% (absolute terms 33–39 ppb) for SE compared to 18–29% (31–36 ppb) over US.

In conclusion, even though the aircraft sampling is fairly representative for the larger scale picture, care has to be taken in extrapolating information from the observations. The goal of the campaign was to actively seek out pollution plumes as forecasted by models and satellite products. This does suggest a positive bias in the dataset over the regional average, as was confirmed in our study, and subsequently would lead to a positive bias if regional estimates are based on solely the aircraft data. For example, quantifying the inflow of pollution to the US from just the aircraft data could lead to a slight overestimate in the influence from Asian airmasses.

4 Summary

Inter-annual variability in background tropospheric CO levels is largely driven by variations in emissions (anthropogenic and natural), transport pathways and photochemistry. Understanding this variability is essential for quantifying contributions of intercontinental transport on local air quality. In this study we analyze aircraft measurements of CO taken during the INTEX-B aircraft campaign in spring 2006 together with satellite retrievals of CO from the MOPITT instrument for 2000–2006 and accompanying model simulations to (1) compare pollutant transport in 2006 to previous years, (2) quantify contributions from changes in emissions, transport pathways and atmospheric oxidiz-

ACPD
9, 17817–17849, 2009

ing capacity on interannual variability, and (3) analyze the representativeness of the aircraft data.

We find that transpacific pollution in spring of 2006 represents a fairly typical scenario in the context of the previous six years. The aircraft sampling does give a fairly good representation for the large-scale picture, however with a larger contribution from Asian sources due to the objective for sampling Asian plumes.

Interannual variability in the total tropospheric CO loading during springtime is of the order 4% and it is estimated that ~1/3 of the variability over the US can be explained by changes in emissions, while ~2/3 is explained by changes in meteorology. Over the Pacific Ocean we estimate that changes in emissions and changes in meteorology contribute with roughly equal proportion. Thus, interannual variability in tropospheric CO loading due to changes in meteorology is an important factor that needs to be considered in analyzing emission trends. Even though CO from fossil fuel and biofuel sources in general makes the largest contribution to CO from direct emission sources, biomass burning sources account for the major part of interannual variability due to their much larger year-to-year changes.

Acknowledgements. The authors acknowledge H. Worden and S. Massie for valuable input to the manuscript. We further acknowledge the INTEX-B teams for providing an extensive and unique set of measurements. The work was supported by NASA grants EOS/03-0601-0145 and NNG04GA459. NCAR is operated by the University Corporation of Atmospheric Research under sponsorship of the National Science Foundation.

References

Bey, I., Jacob, D. J., Logan, J. A., and Yantosca, R. M.: Asian chemical outflow to the Pacific: origins, pathways and budgets, J. Geophys. Res., 106, 23097–23114, 2001.

Deeter, M. N., Emmons, L. K., Edwards, D. P., Gille, J. C., and Drummond, J. R.: Vertical resolution and information content of CO profiles retrieved by MOPITT, Geophys. Res. Lett., 31, L15112, doi:10.1029/2004GL020235, 2004.

Deeter, M. N., Edwards, D. P., and Gille, J. C.: Retrievals of Carbon Monoxide profiles from MOPITT observations using log-normal a priori statistics, J. Geophys. Res., 112, D11311, doi:10.1029/2006JD007999, 2007,

Drummond, J. R. and Mand, G. S.: The Measurements of Pollution in the Troposphere (MOPITT) instrument: Overall performance and calibration requirements, J. Atmos. Ocean. Techn., 13, 314–320, 1996.

Emmons, L. K., Edwards, D. P., Deeter, M. N., Gille, J. C., Campos, T., Nédélec, P., Novelli, P., and Sachse, G.: Measurements of Pollution In The Troposphere (MOPITT) validation through 2006, Atmos. Chem. Phys., 9, 1795–1803, 2009a, http://www.atmos-chem-phys.net/9/1795/2009/.

Emmons, L. K., Walters, S., Hess, P. G., Lamarque, J.-F., Pfister, G. G., Fillmore, D., Granier, C., Guenther, A., Kinnison, D., Laepple, T., Orlando, J., Tie, X., Tyndall, G., Wiedinmyer, C., Baughcum, S. L., and Kloster, S.: Description and evaluation of the Model for Ozone and Related chemical Tracers, version 4 (MOZART-4), Geosci. Model Dev. Discuss., 2, 1157–1213, 2009b.

Emmons, L. K., Pfister, G. G., Edwards, D. P., et al.: Measurements of Pollution in the Troposphere (MOPITT) Validation exercises during summer 2004 field campaigns over North America, J. Geophys. Res., 112, D12S02, doi:10.1029/2006JD007833, 2007.

Emmons, L. K., Deeter, M. N., Gille, J. C., et al.: Validation of Measurements of Pollution in the Troposphere (MOPITT) CO retrievals with aircraft in-situ profiles, J. Geophys. Res., 109, D03309, doi:10.1029/2003JD004101, 2004.

Gerbig, C., Schmitgen, S., Kley, D., Volz-Thomas, A., Dewey, K., and Haaks, D.: An improved fast-response vacuum-UV resonance fluorescence CO instrument, J. Geophys. Res., 104, 1699–1704, 1999.

Goldstein, A. H., Millet, D. B., McKay, M., Jaegle, L., Horowitz, L., Cooper, O., Hudman, R., Jacob, D. J., and Oltsman, S.: Impact of Asian emissions on observations at Trinidad Head, California during ITCT 2K2, J. Geophys. Res., 109, D23S17, doi:10.1029/2003JD004406, 2004.

Horowitz, L., Walters, S., Mauzerall, D. L., Emmons, L. K., Rasch, P. J., Granier, C., Tie, X., Lamarque, J.-F., Schultz, M. G., Tyndall, G. S., Orlando, J. J., and Brasseur, G. P.: A global simulation of tropospheric ozone and related tracers: Description and evaluation of MOZART, version 2, J. Geophys. Res., 108(D24), 4784, doi:10.1029/2002JD002853, 2003.

Jaffe, D., Bertschi, I., Jaegle, L., Novelli, P., Reid, J. S., Tanimoto, H., Vingarzan, R.,

and Westphal, D. L.: Long-range transport of Siberian biomass burning emissions and impact on surface ozone in Western North America, Geophys. Res. Lett., 31, L16106, doi:10.1029/3004GL020093, 2004.

Liu, H., Jacob, D. J., Bey, I., Yantosca, R. M., Duncan, B., and Sachse, G. W.: Transport pathways for Asian pollution outflow over the Pacific: Interannual and seasonal variations, J. Geophys. Res., 108(D20), 8786, doi:10.1029/2202JD003102, 2003.

Merritt, M. N., Edwards, D. P., Gille, J. C., et al.: The MOPITT Version 4 CO Product: Algorithm Enhancements, Validation and Long-Term Stability, J. Geophys. Res., submitted, 2009.

Newell, R. E. and Evans, M. J.: Seasonal changes in pollutant transport to the North Pacific: the relative importance of Asian and European sources, Geophys. Res. Letters, 27(16), 2509–2512, 2000.

Ohara, T., Akimoto, H., Kurokawa, J., Horii, N., Yamaji, K., Yan, X., and Hayasaka, T.: An Asian emission inventory of anthropogenic emission sources for the period 1980–2020, Atmos. Chem. Phys., 7, 4419–4444, 2007, http://www.atmos-chem-phys.net/7/4419/2007/.

Olivier, J., Peters, J., Granier, C., et al.: Present and future surface emissions of atmospheric compounds, European Commission report EVK2 199900011, available at: http://tropo.aeronomie.be/pdf/POET_emissions_report.pdf, 2004.

Park, I. S., Choi, W. J., Lee, T. Y., Lee, S. J., Han, J. S., and Kim, C. H.: Simulation of long-range transport of air pollutants over Northeast Asia using a comprehensive acid deposition model, Atmos. Environ., 39, 4075–4085, 2005.

Parrish, D. D., Kondo, Y., Cooper, O. R., Brock, C. A., Jaffe, D. A., Trainer, M., Ogawa, T., Huebler, G., and Fehsenfeld, F. C.: Intercontinental Transport and Chemical Transformation 2002 (ITCT 2K2) and Pacific Exploration of Asian Continental Emissions (PEACE) experiments: An overview of the 2002 winter and spring intensives, J. Geophys. Res., 109, D23S01, doi:10.1029/2004JD004980, 2004.

Pfister, G., Emmons, L. K., Hess, P. G., Lamarque, J.-F., Walters, S., Guenther, A., Palmer, P. I., and Lawrence, P.: Contribution of isoprene to chemical budgets: A model tracer study with the NCAR CTM MOZART-4, J. Geophys. Res., 113, D05308, doi:10.1029/2007JD008948, 2008.

Sachse, G. W., Hill, G. F., Wade, L. O., and Perry, M. G.: Fast response, high precision carbon monoxide sensor using a tunable diode laser absorption technique, J. Geophys. Res., 92, 2071–2081, 1987.

Singh, H. B., Brune, W. H., Crawford, J. H., Flocke, F., and Jacob, D. J.: Chemistry and transport of pollution over the Gulf of Mexico and the Pacific: spring 2006 INTEX-B campaign overview and first results, Atmos. Chem. Phys., 9, 2301–2318, 2009, http://www.atmos-chem-phys.net/9/2301/2009/.

Szopa, S., Hauglustaine, D. A., and Ciais, P.: Relative contributions of biomass burning emissions and atmospheric transport to carbon monoxide interanual variability, Geophys. Res. Letters, 35, L01401, doi:10.1029/2007GL030231, 2007.

Tie, X., Brasseur, G., Emmons, L., Horowitz, L., and Kinnision, D.: Effects of aerosols on tropospheric oxidants: A global model study, J. Geophys. Res., 106, 2931–2964, 2001.

Tie, X., Madronich, S., Walters, S., Edwards, D. P., Ginoux, P., Mahowald, N., Zhang, R., Luo, C., and Brasseur, G.: Assessment of the global impact of aerosols on tropospheric oxidants, J. Geophys. Res., 110, D03204, doi:10.1029/2004JD005359, 2005.

van der Werf, G. R., Randerson, J. T., Giglio, L., Collatz, G. J., Kasibhatla, P. S., and Arellano Jr., A. F.: Interannual variability in global biomass burning emissions from 1997 to 2004, Atmos. Chem. Phys., 6, 3423–3441, 2006, http://www.atmos-chem-phys.net/6/3423/2006/.

Wang, Y., Choi, Y., Zeng, T., Ridley, B., Blake, N., Blake, D., and Flocke, F.: Late-spring increase of trans-Pacific pollution transport in the upper troposphere, Geophys. Res. Lett., 33, L01811, doi:10.1029/2005GL024975, 2006.

Zhang, Q., Streets, D. G., Carmichael, G. R., He, K. B., Huo, H., Kannari, A., Klimont, Z., Park, I. S., Reddy, S., Fu, J. S., Chen, D., Duan, L., Lei, Y., Wang, L. T., and Yao, Z. L.: Asian emissions in 2006 for the NASA INTEX-B mission, Atmos. Chem. Phys., 9, 5131–5153, 2009, http://www.atmos-chem-phys.net/9/5131/2009/.

Table 1. Emission totals for CO (Tg CO) for March–May of the individual years. Values in parenthesis give the percentage difference relative to the 6 yr mean. Totals are calculated for different regions and different emission source types (all emissions, FF, BB, BIO).

Year	CO all	CO BB	CO FF	CO BIO
N-Hemisphere				
2000	245 (99%)	60 (106%)	156 (96%)	24.4 (100%)
2001	238 (96%)	51 (91%)	158 (97%)	24.4 (100%)
2002	237 (96%)	48 (84%)	160 (99%)	24.4 (100%)
2003	280 (113%)	89 (157%)	164 (101%)	24.4 (100%)
2004	249 (101%)	55 (98%)	165 (102%)	24.4 (100%)
2005	241 (97%)	46 (81%)	166 (102%)	24.4 (100%)
2006	241 (98%)	46 (82%)	167 (103%)	24.4 (100%)
Asia (0–90° N, 60–160° E)				
2000	110 (89%)	29 (79%)	72 (92%)	7.6 (100%)
2001	121 (98%)	39 (106%)	73 (94%)	7.6 (100%)
2002	116 (94%)	32 (87%)	76 (97%)	7.6 (100%)
2003	143 (116%)	53 (146%)	80 (102%)	7.6 (100%)
2004	131 (106%)	42 (116%)	81 (104%)	7.6 (100%)
2005	121 (99%)	31 (84%)	82 (105%)	7.6 (100%)
2006	121 (98%)	30 (82%)	82 (106%)	7.6 (100%)
N-America (30–90° N, 180–60° W)				
2000	40 (100%)	1.1 (105%)	34 (100%)	4.9 (100%)
2001	40 (99%)	0.8 (77%)	34 (100%)	4.9 (100%)
2002	41 (102%)	1.5 (151%)	34 (100%)	4.9 (100%)
2003	40 (100%)	0.7 (73%)	34 (100%)	4.9 (100%)
2004	40 (100%)	0.9 (88%)	34 (100%)	4.9 (100%)
2005	40 (100%)	1.0 (97%)	34 (100%)	4.9 (100%)
2006	40 (100%)	1.1 (109%)	34 (100%)	4.9 (100%)
C-America (0–30° N, 180–60° W)				
2000	34 (193%)	23 (193%)	8 (100%)	3.3 (100%)
2001	18 (76%)	6 (52%)	8 (100%)	3.3 (100%)
2002	18 (79%)	7 (56%)	8 (100%)	3.3 (100%)
2003	37 (162%)	28 (233%)	8 (100%)	3.3 (100%)
2004	15 (66%)	4 (31%)	8 (100%)	3.3 (100%)
2005	20 (88%)	9 (75%)	8 (100%)	3.3 (100%)
2006	18 (80%)	7 (59%)	8 (100%)	3.3 (100%)

ACPD
9, 17817–17849, 2009

Table 2. Deviation from the 6 yr mean (Tg) for the total and tagged CO burden per year (2001 is excluded to match the time period of MOPITT data) and per region as well as mean absolute burden (MTB; Tg) for total CO and the different tags. For comparison to MOPITT, the burden is calculated over the altitude range 800–300 mbar. Tags are grouped into six source regions (EuAf–Europe and N-Africa; SWas–SW-Asia; SEas–SE-Asia; NAs–N-Asia; NAm–N-America; CAm–C-America) or three source types (BB–Biomass Burning; FF–Fossil Fuel and Biofuel; Bio–Biogenic). Untagged sources are listed in the last column (Rest). Numbers in bold highlight negative values.

Pacific											
	CO	EuAf	SWas	SEas	NAs	NAm	CAm	BB	FF	Bio	Rest
2000	**−1.64**	**−0.01**	**−0.52**	**−0.83**	**−0.14**	0.04	0.20	**−0.26**	**−0.96**	**−0.04**	**−0.38**
2002	**−1.38**	0.05	**−0.19**	**−0.50**	**−0.48**	**−0.09**	**−0.13**	**−0.61**	**−0.70**	**−0.02**	**−0.05**
2003	1.66	**−0.21**	**−0.10**	**−0.23**	1.67	0.01	0.29	1.40	0.05	0.00	0.22
2004	1.21	0.17	0.82	0.61	**−0.43**	**−0.01**	**−0.15**	0.38	0.60	0.03	0.20
2005	0.10	**−0.09**	**−0.05**	0.66	**−0.43**	**−0.03**	**−0.06**	**−0.46**	0.45	0.01	0.09
2006	0.05	0.09	0.04	0.27	**−0.19**	0.08	**−0.15**	**−0.47**	0.58	0.02	**−0.09**
MTB	30.73	4.22	3.24	5.89	1.23	2.57	0.74	3.80	12.84	1.24	12.85
US											
	CO	EuAf	SWas	SEas	NAs	NAm	CAm	BB	FF	Bio	Rest
2000	**−0.61**	0.02	**−0.20**	**−0.33**	**−0.08**	**−0.17**	0.26	0.04	**−0.52**	**−0.03**	**−0.11**
2002	**−0.94**	0.03	**−0.17**	**−0.24**	**−0.16**	**−0.33**	**−0.06**	**−0.24**	**−0.64**	**−0.05**	**−0.01**
2003	1.03	**−0.06**	**−0.01**	**−0.02**	0.66	0.11	0.23	0.58	0.29	0.04	0.12
2004	0.12	0.03	0.34	0.21	**−0.19**	**−0.13**	**−0.17**	0.17	**−0.05**	**−0.02**	0.03
2005	0.51	0.03	0.03	0.32	**−0.15**	0.36	**−0.12**	**−0.23**	0.65	0.05	0.04
2006	**−0.13**	**−0.03**	0.03	0.05	**−0.10**	0.16	**−0.16**	**−0.33**	0.28	0.01	**−0.08**
MTB	18.92	2.43	1.67	3.09	0.53	3.04	0.68	2.09	8.48	0.88	7.47

ACPD
9, 17817–17849, 2009

Table 3. Average model tracer and total CO concentrations (ppb) over 2 km wide altitude bins. Averages for April and May 2006 are calculated for model data interpolated to C-130 flights and for SEattle region.

Alt (km)	FF^{ASIA}		BB^{ASIA}		NAm		CAm		EuAf		Bio		Chem		Total	
	C130	Seattle	C130	Seattle	C130	Seattle	C130	Seattle	C130	Seattle	C130	Seattle	C130	Seattle	C130	Seattle
1	32	32	6	7	33	25	2	2	25	23	10	8	53	52	**160**	**148**
3	34	32	7	8	15	14	2	2	21	19	6	6	50	50	**135**	**131**
5	34	33	7	8	13	13	2	2	18	18	6	5	49	50	**129**	**128**
7	41	33	7	8	13	13	2	2	18	18	6	5	48	48	**137**	**123**

ACPD

9, 17817–17849, 2009

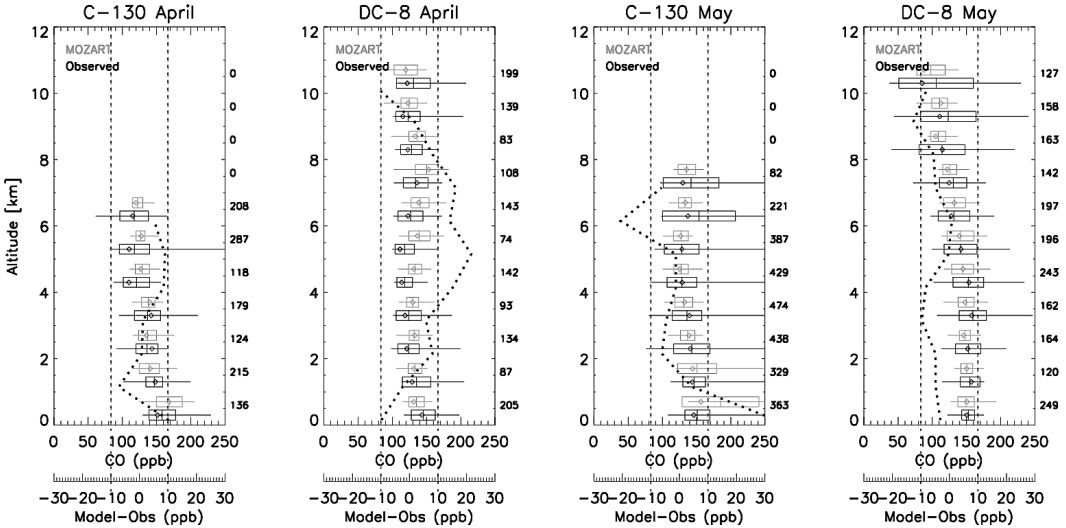

Fig. 1. Comparison of MOZART CO fields with aircraft observations from the C-130 and the DC-8 during INTEX-B (only science flights included. Bar plots represent mean, median, standard deviation, minimum and maximum values for observed and modeled CO concentrations averaged over 1 km altitude bins. The thick dotted line gives the difference between modeled and observed values and thin vertical dotted lines indicate grid lines for difference values of ±10 ppb.

ACPD
9, 17817–17849, 2009

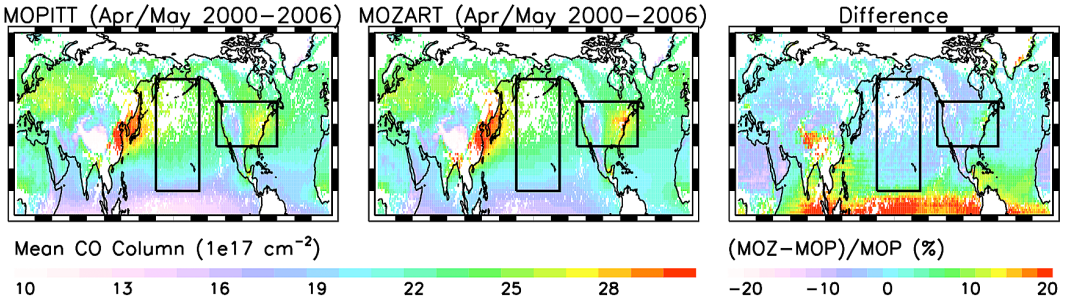

Fig. 2. Northern Hemispheric MOPITT and MOZART (with MOPITT averaging kernels applied) springtime CO columns averaged over the years 2000–2006 (excluding 2001) and their relative difference (%). (Data for daytime and a priori fractions <50%). The rectangles indicate the two regions of interest: PAC and US.

ACPD
9, 17817–17849, 2009

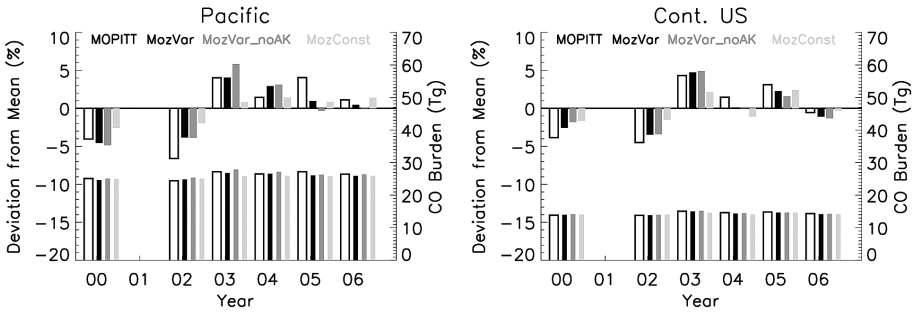

Fig. 3. Variability in the tropospheric springtime (April–May) CO burden (relative deviation from mean (top bars) and absolute amounts (bottom bars)) over PAC and US as derived from MOPITT (open bars) data and the model simulations MozVar and MozConst (filled bars). MozVar results are shown when modeled fields are convoluted with MOPITT averaging kernels and also when the burden is calculated from the raw model data. The higher burden for PAC compared to US is explained by the larger area. Average area normalized burden for PAC is 9.09×10^{-7} Tg/km^2 and for US 9.32×10^{-7} Tg/km^2.

ACPD
9, 17817–17849, 2009

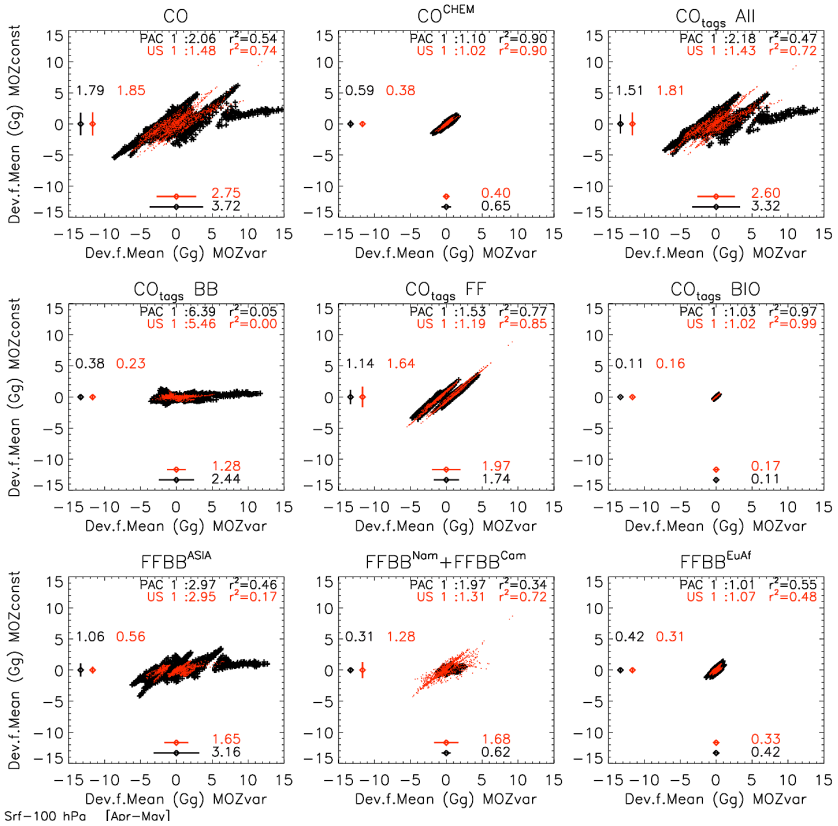

Fig. 4. Interannual deviations from 7 yr mean [Gg CO] for each gridbox over PAC (black) and US (red). Results for MozVar plotted versus MozConst for the springtime tropospheric burden (surface-100 mbar) of total, chemically produced and tagged CO. The relative ratio of the standard deviation in MozConst versus MozVar and also the correlation coefficients are indicated in the plots. Symbols in the center of the x- and y-axis indicate the standard deviation.

ACPD
9, 17817–17849, 2009

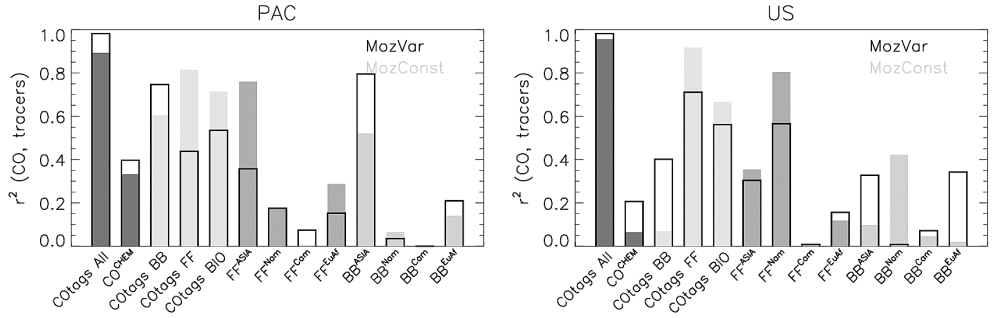

Fig. 5. Correlation (r^2) between the absolute deviation from mean in total CO burden and the different CO contributions over PAC and US. Results for MozVar (open bars) and MozConst (filled bars). r^2 is calculated from the springtime (April–May average) burden (surface-100 mbar) for each grid cell within the region of interest for the years 2000–2006.

ACPD
9, 17817–17849, 2009

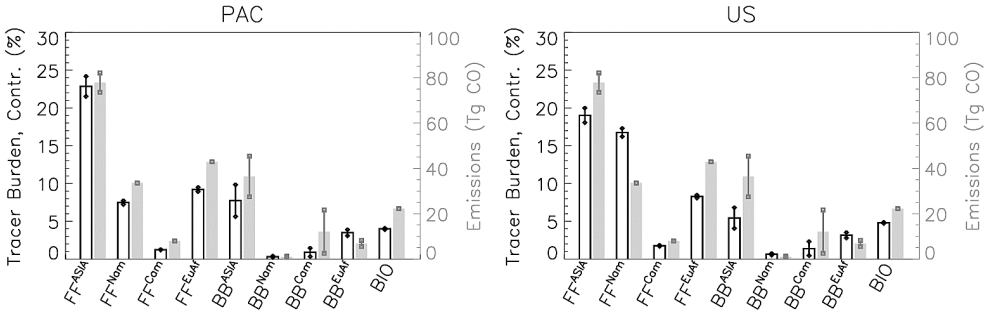

Fig. 6. Mean (column) and standard deviation (error bars) of tracer contributions to the total CO burden (surface-100 mbar; open bars) over PAC and US as well as emissions for individual tracers (filled bars) for 2000–2006. Tracer burden is integrated over April–May, the emissions over March–May. Note the emissions are the same in both graphs.

ACPD
9, 17817–17849, 2009

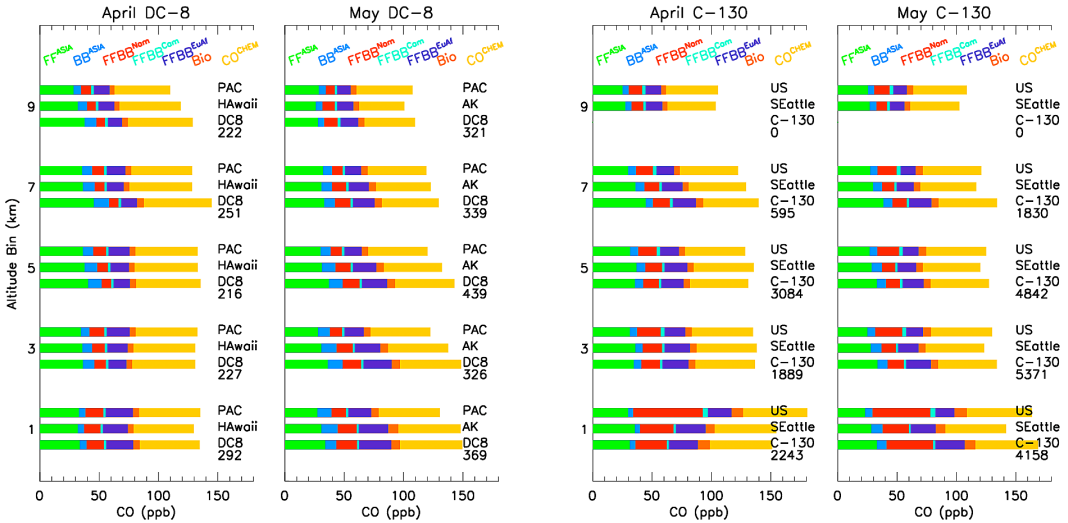

Fig. 7. Average tracer CO concentrations (ppb) for April and May 2006. Results are given for DC-8 and C-130 flight tracks, regions representative for flight coverage (Hawaii and Alaska (AK) for the DC-8 flights in April and May, respectively and Seattle area for C-130 flights) and for the two larger regions PAC and US. Results are shown for 2 km wide altitude bins. The number of observations per bin is listed.

ACPD
9, 17817–17849, 2009

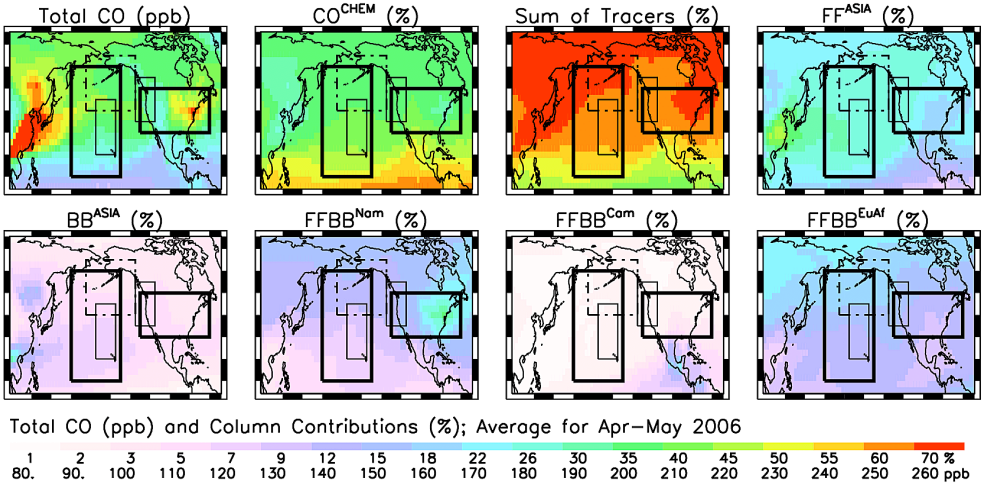

Fig. 8. Average Column Total CO Mixing Ratio for 0–10 km and Relative Tracer Contributions. The boxes indicate the different regions: HA, AK, PAC, SE and US.

ACPD
9, 17817–17849, 2009